ANNALS OF PHYSICS 99, 164–187 (1976)

Influence of Anomalous Thresholds in Electron-Positron Annihilation into Hadrons: The $e^+e^- \to \rho\pi\pi$ Cross Section

G. KRAMER

II. *Institut für Theoretische Physik der Universität, Hamburg*

G. SCHIERHOLZ

CERN, Geneva

AND

K. SUNDERMEYER

Gesamthochschule Wuppertal, Fachbereich Physik, Wuppertal

We calculate the cross section for $e^+e^- \to \rho\pi\pi$ on the basis of partial-wave dispersion relations in the $\pi\pi$ channel taking proper account of anomalous singularity contributions. The appearance of anomalous thresholds is due to the fact that the vertex $\gamma_V\rho(\pi\pi)$ becomes internally unstable as the virtual photon mass is increased. Reasonable agreement with existing data is found. The anomalous singularity contributions provide by far the dominant part of the cross section which is a warning to using naive vector dominance extrapolations in estimating the electron–positron cross section.

1. INTRODUCTION

Recently a series of experiments on e^+e^--annihilation into hadrons at Frascati and SLAC have produced data on $e^+e^- \to \pi^+\pi^-\pi^+\pi^-$ at center-of-mass energies $(q^2)^{1/2}$ between 1 and 5 GeV [1]. The cross section for $e^+e^- \to 4\pi^\pm$ shows a broad peak centered at $(q^2)^{1/2} = 1.6$ GeV and falls off with increasing q^2 like q^{-6} [1]. A quite similar enhancement in the four-pion system around 1.6 GeV has also been seen in the high-energy photoproduction process $\gamma p \to \pi^+\pi^-\pi^+\pi^- p$ [2]. Both phenomena are usually interpreted as the production of a $J^{PC} = 1^{--}$ resonance, called ρ', which is directly coupled to the photon and decays predominantly into $2\pi^+2\pi^-$ [3]. Then the reaction $\gamma p \to 2\pi^+2\pi^- p$ can proceed through the usual VDM type mechanism. Actually in both experiments it was found that the $2\pi^+2\pi^-$ mass enhancement is dominated by the $\rho^0\pi^+\pi^-$ state [1, 2]. It is well known that the ρ' interpretation of these experiments is not unique [4].

An explanation equally applicable to e^+e^- annihilation and to photoproduction is the opening of quasi-two-body decay modes of the ρ^0 which produces bumps right after their threshold, e.g., $\rho^0 \to \rho^0\epsilon$, $\rho^0 \to \rho^0 f$, $\rho^0 \to \pi^\pm A_1^\mp$ etc. [5–7]. In particualr, in [7] it was shown that the experimental $2\pi^+2\pi^-$ mass distribution in $e^+e^- \to 2\pi^+2\pi^-$ and $\gamma p \to 2\pi^+2\pi^- p$ could well be fitted in an isobaric model for $\gamma \to \rho^0\pi^+\pi^-$, where the photon couples directly to the ρ^0 and an $I = J = 0$ resonance, the ϵ, which occurs in the $\pi^+\pi^-$ channel. The absolute value of the cross section could not be calculated since the couplings of the ρ^0 to the $\rho^0\epsilon$ system are essentially unknown. Only if one of the $\rho^0\rho^0\epsilon$ couplings was related using VDM to the $\epsilon\gamma\gamma$ coupling, which had been calculated in a recent dynamical model [8], it turned out that the coupling was of the right order to reproduce the measured cross section for $e^+e^- \to \rho^0\pi^+\pi^-$. This procedure was unsatisfactory in two respects. First the coupling of the ρ^0 to the $\rho^0\epsilon$ system depends on two independent coupling constants. Only one of them occurs in the coupling of the real photon to the $\gamma\epsilon$ system. Second it is rather doubtful that the extrapolation in the vector meson masses squared from $q^2 = 2.5\ \mathrm{GeV}^2$ and $p_1^2 = m_\rho^2$, respectively, to $q^2 = p_1^2 = 0$ (see Fig. 1 for the notation of momenta) for both vector mesons is well represented by the naive VDM approach. Both ρ^0's and the ϵ can decay into two pions. Therefore in all three mass variables of the $\rho^0\rho^0\epsilon$ vertex two-pion intermediate states occur which lead to anomalous thresholds in the respective variables if the others are above $2m_\pi^2$.

In this paper we consider the matrix element for $\gamma \to \rho^0\pi^+\pi^-$ as a function of s, the $\pi^+\pi^-$ invariant mass squared, and for fixed angular momentum states in the 2π system so that we encounter anaomalous singularities in this variable for the partial wave amplitudes. The virtual photon mass is also allowed to vary but the partial wave dispersion relations are written in s and not in q^2. This way it is possible to take into account the full variation of the two-pion s-wave phase shift.

The framework of our calculations is similar to an earlier work, done by two of us, for the reaction $\gamma\gamma \to \pi^+\pi^-$ with two real photons [8]. We use dispersion relations for the partial waves of $\gamma \to \rho^0\pi^+\pi^-$ in the $\pi^+\pi^-$ channel. The left-hand cut is approximated by π and ω exchange while on the right-hand cut we assume elastic unitarity. Here we restrict ourselves to the $I = J = 0$ contribution in the vicinity of the ϵ mass. Using a Breit–Wigner parametrization for the phase shift we calculate the form factors for $\gamma \to \rho^0\epsilon$ as a function of q^2. Of course, the derived equations can be used also for other partial waves and for other input phase shifts than the usual resonance parametrizations. But their numerical evaluation would be beyond the scope of this paper. The outline of the paper is as follows. In Section 2 we discuss the kinematical decomposition of the matrix elements and the relevant formulas for the calculation of form factors and cross sections. In Section 3 the dispersion relations are introduced and the anomalous cut contributions derived. In Section 4 we describe our input assumptions concerning the $\pi\pi$ phase shifts

and present and discuss the results of our calculations. Finally Section 5 is left for some concluding remarks.

2. Decomposition of the Matrix Elements

To introduce the final state interactions in the two-pion system of $\rho^0\pi^+\pi^-$ based on unitarity and dispersion relations, we work in the two pion center-of-mass system $\mathbf{p}_2 + \mathbf{p}_3 = 0$. The notation of the kinematic variables is shown in Fig. 1.

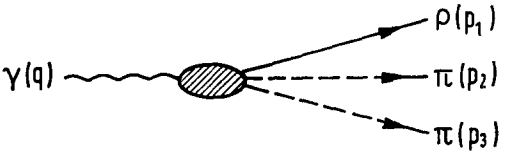

FIG. 1. Kinematic diagram for $\gamma \to \rho\pi\pi$.

To control the kinematic singularities we also introduce invariant amplitudes $A_i(s, t)$. The decomposition of the matrix element for $\gamma \to \rho^0\pi^+\pi^-$ in terms of the $A_i(s, t)$ $(i = 1,..., 5)$ was introduced in [7] and will not be repeated here. The next step is to relate the s-channel helicity amplitudes (in the system $\mathbf{p}_2 + \mathbf{p}_3 = 0$) to the invariant amplitudes A_i. The s-channel helicity amplitudes are defined by:

$$\begin{aligned} T_{\lambda_1\kappa} &= \langle p_1, \lambda_1, p_2, p_3 \mid J_\nu(0) \mid 0\rangle\, e^\nu(\kappa) \\ &= e^\mu(\lambda_1)^*\, T_{\mu\nu} e^\nu(\kappa) \end{aligned} \tag{2.1}$$

where λ_1, κ are the helicities of the ρ meson and the virtual photon, respectively. The $T^i_{\mu\nu}$ are decomposed into gauge invariant covariants $F_{\mu\nu}$, defined in [7],

$$T_{\mu\nu} = \sum_{i=1}^{5} A_i(s, t)\, F^i_{\mu\nu}. \tag{2.2}$$

From (2.1) the s-channel helicity amplitudes can be expressed by the invariant amplitudes, i.e.,

$$T_{\lambda_1\kappa} = \sum_{i=1}^{5} A_i(s, t)\, g^i_{\lambda_1\kappa} \tag{2.3}$$

where

$$g^i_{\lambda_1\kappa} = e^\mu(\lambda_1)^*\, F^i_{\mu\nu} e^\nu(\kappa). \tag{2.4}$$

The $g^i_{\lambda_1\kappa}$ are listed in Appendix A together with the definitions of the Mandelstam variables s, t, u.

The s-channel helicity amplitudes are decomposed into partial waves:

$$T_{\lambda_1\kappa} = \sum_j (2j+1)\, T^j_{\lambda_1\kappa}(s)\, d^j_{\lambda_1-\kappa,0}(\theta) \tag{2.5}$$

where θ is the angle between $\mathbf{q}$ and $\mathbf{p}_2$ in the system $\mathbf{q} = \mathbf{p}_1$.

For the matrix element $\gamma \to \rho^0\epsilon$ we use the following decomposition:

$$\begin{aligned}
&\langle \epsilon(p_a), \rho^0(p_b, \mu) | J_\nu(0) | 0 \rangle \\
&\quad = G_1(q^2)(p_b q g_{\mu\nu} - q_\mu p_{b\nu}) \\
&\qquad + G_2(q^2)([(p_b q)^2 - p_b{}^2 q^2]\, g_{\mu\nu} + p_b{}^2 q_\mu q_\nu + q^2 p_{b\mu} p_{b\nu} - (p_b q)(p_{b\mu} q_\nu + q_\mu p_{b\nu}))
\end{aligned} \tag{2.6}$$

where $q = p_b + p_a$. The definition of these invariant transition form factors G_1 and G_2 for $\gamma \to \rho^0\epsilon$ differs from the definitions used earlier [6]. The tensor (2.6) is divergenceless concerning multiplication with q^ν but also concerning multiplication with $p_b{}^\mu$. In order to obtain the transition matrix elements for the usual polarisation states of the ρ^0 we must multiply (2.6) with the appropriate polarization vectors $e^\mu(\lambda_1)$. With (2.6) we calculate the helicity form factors F^{λ_1} for $\gamma \to \rho^0\epsilon$ in the system $\mathbf{q} = 0$, introduced in [6].

The relations between the transverse and longitudinal form factor F^1 and F^0 and the invariant form factors G_1 and G_2 are:

$$\begin{aligned}
F^1 &= G_1 p_b q + G_2((p_b q)^2 - p_b{}^2 q^2) \\
F^0 &= (q^2 p_b{}^2)^{1/2}\, G_1 .
\end{aligned} \tag{2.7}$$

These two helicity form factors determine the cross section for $e^+e^- \to \rho^0\epsilon$, i.e., [6]

$$d\sigma/d\cos\theta = \frac{\alpha\, |\, \mathbf{p}_a\, |}{8(q^2)^{5/2}} \{ |\, F^0\, |^2 \sin^2\theta + |\, F^1\, |^2 (1 + \cos^2\theta) \} \tag{2.8}$$

where θ is the angle between the momentum of the ϵ resonance and the direction of the incoming positron, $|\, \mathbf{p}_a\, |$ is the momentum of the ϵ in the e^+e^- center-of-mass system.

The contribution of the ϵ resonance to the invariant amplitudes is

$$\begin{aligned}
A_1 &= \frac{1}{s - m_\epsilon{}^2 + i m_\epsilon \Gamma_\epsilon}\, g_{\epsilon\pi\pi}(G_1 + (qp_1)\, G_2) \\
A_5 &= \frac{-1}{s - m_\epsilon{}^2 + i m_\epsilon \Gamma_\epsilon}\, g_{\epsilon\pi\pi} G_2 \\
A_2 &= A_3 = A_4 = 0.
\end{aligned} \tag{2.9}$$

The corresponding s-channel helicity amplitudes are:

$$T_{00} = \frac{1}{m_\epsilon^2 - s - im_\epsilon\Gamma_\epsilon} g_{\epsilon\pi\pi}(p_1^2 q^2)^{1/2} G_1$$
$$T_{11} = \frac{1}{m_\epsilon^2 - s - im_\epsilon\Gamma_\epsilon} g_{\epsilon\pi\pi}(p_1 q G_1 + ((p_1 q)^2 - p_1^2 q^2) G_2). \tag{2.10}$$

The other helicity amplitudes vanish for $J = 0$ exchange in the s channel. From (2.10) we can immediately obtain the form factors G_1 and G_2 by evaluating T_{00} and T_{11} at $s = m_\epsilon^2$:

$$G_1 = \frac{m_\epsilon\Gamma_\epsilon}{g_{\epsilon\pi\pi}(p_1^2 q^2)^{1/2}} \operatorname{Im} T_{00}$$
$$G_2 = \frac{m_\epsilon\Gamma_\epsilon}{g_{\epsilon\pi\pi}((p_1 q)^2 - p_1^2 q^2)} \operatorname{Im}\left(T_{11} - \frac{(p_1 q)}{(p_1^2 q^2)^{1/2}} T_{00}\right). \tag{2.11}$$

3. Dispersion Relations and Anomalous Thresholds

The dynamical calculations are similar to the calculations for the process $\gamma\gamma \to \pi\pi$, which have been performed by two of us [8]. Because in $\gamma \to \rho^0\pi\pi$ the q^2 of the virtual photon is timelike in such a way it can decay into real particles we encounter anomalous thresholds. The one-pion exchange in the t- and u-channel is the first to aquire anomalous thresholds. The next anomalous threshold is obtained for 3π exchange in the t- and u-channel. This contribution will be approximated by ω exchange. The anomalous thresholds encountered here are, however, different from those arising from the one-pion exchange. For one-pion exchange the upper ($\gamma \to \pi\pi$) and the lower vertex ($\rho \to \pi\pi$) are unstable. In this case the anomalous cuts are on the real axis. For ω exchange only the upper vertex is unstable ($\gamma \to \omega\pi$) whereas the lower vertex is stable ($\rho \to \omega\pi$). In this case the anomalous thresholds are in the complex plane as will be seen later.

For our calculations we need the partial wave projections of the t- and u-channel contributions. Furthermore we must find out which combinations of the partial wave amplitudes are free of kinematical singularities and what are the other kinematical constraints in particular at the different thresholds (or pseudo-thresholds). As usual we define the partial wave projections of the invariant amplitudes $A_i(s, t)$:

$$A_i^j(s) = \tfrac{1}{2}\int_{-1}^{+1} d\cos\theta A_i(s, t)\, d_{00}^j(\cos\theta). \tag{3.1}$$

The relations between the partial-wave projections of the helicity amplitudes and the A_i^j are easily derived with the help of the formulas in Appendix A.

In this paper we need only the s-wave amplitudes. For them the decomposition is:

$$T_{11}^0 = -(p_1q)\,A_1{}^0 + ((p_1q) - \mathbf{q}^2)\,\mathbf{p}_2{}^2\tfrac{4}{3}A_2{}^0 - ((p_1q) + 2\mathbf{q}^2)\,\mathbf{p}_2{}^2\tfrac{4}{3}A_2{}^2 + 2\,|\,\mathbf{p}_2\,|\,|\,\mathbf{q}\,|\,(q^2A_3{}^1 + p_1{}^2A_4{}^1) - p_1{}^2q^2A_5{}^0 \tag{3.2}$$

$$T_{00}^0 = (q^2p_1{}^2)^{1/2}\{-A_1{}^0 + \tfrac{4}{3}\mathbf{p}_2{}^2A_2{}^0 + \tfrac{8}{3}\mathbf{p}_2{}^2A_2{}^2 + 2\,|\,\mathbf{p}_2\,|\,|\,\mathbf{q}\,|\,(A_3{}^1 + A_4{}^1) - (p_1q)\,A_5{}^0\}.$$

All other s-wave helicity amplitudes vanish. The $A_i{}^j$ can be calculated from a fixed-s dispersion relation. Then $A_i{}^j \sim (|\,\mathbf{p}_2\,|\,|\,\mathbf{q}\,|)^j$ if $|\,\mathbf{p}_2\,| \to 0$ or $|\,\mathbf{q}\,| \to 0$ for those parts of the A_i for which the t-channel or u-channel exchanges are stable concerning the decay into $\rho^0\pi^\pm$. This is, for example, fulfilled for pion exchange. Then T_{11}^0 and T_{00}^0 obey constraints for $|\,\mathbf{q}\,| \to 0$, i.e., $p_1q = \pm(p_1{}^2q^2)^{1/2}$. For example, we have in the limit $|\,\mathbf{q}\,| = 0$:

$$T_{11}^0 \pm T_{00}^0 = (p_1q \pm (p_1{}^2q^2)^{1/2})(-A_1{}^0 + \tfrac{4}{3}\mathbf{p}_2{}^2A_2{}^0 \mp (p_1{}^2q^2)^{1/2}\,A_5{}^0), \tag{3.3}$$

i.e., $T_{11}^0 + T_{00}^0$ must vanish for $p_1q = -(p_1{}^2q^2)^{1/2}$ or $s = ((p_1{}^2)^{1/2} + (q^2)^{1/2})^2$ and $T_{11}^0 - T_{00}^0$ must vanish for $p_1q = (p_1{}^2q^2)^{1/2}$ or $s = ((p_1{}^2)^{1/2} - (q^2)^{1/2})^2$. Therefore we write down subtracted dispersion relations for $T_{11}^0 \pm T_{00}^0$ with subtraction points $s = ((p_1{}^2)^{1/2} \pm (q^2)^{1/2})^2$, respectively. This way we fulfill the necessary threshold conditions in connection with pion and ω exchange. At the threshold $|\,\mathbf{p}_2\,| = 0$ a similar constraint as for $|\,\mathbf{q}\,| = 0$ does not exist.

With (3.2) it is easy to calculate the contributions of π and ω exchange to $T_{11}^0 \pm T_{00}^0$. The invariant amplitudes for these two exchanges have been given in [7]. To avoid complications with the bad asymptotic behavior of elementary vector meson exchange we follow [8] and assume that the ω lies on a Regge trajectory α_ω. Otherwise further subtractions are necessary in the partial-wave dispersion relations. The reggeization of the ω exchange with the help of the Khuri representation in order to incorporate the lowest thresholds imposed by the boundary of the diagram in Fig. 2 amounts to a multiplication of the elementary ω-exchange term with a form factor F of the following form (see [8]):

$$F = \exp((\alpha_\omega(t) - 1)\,\xi(s)) \tag{3.4}$$

where

$$\begin{aligned}
\xi(s) &= \operatorname{arc\,cosh} z_{t=b(s)} \\
z_t &= \{2s + t - 2m_\pi{}^2 - q^2 - m_\rho{}^2 + (m_\rho{}^2 - m_\pi{}^2)(q^2 - m_\pi{}^2)/t\}/4p_{13}p_{24} \\
p_{13}^2 &= (t - ((q^2)^{1/2} - m_\pi)^2)(t - ((q^2)^{1/2} + m_\pi)^2)/4t \\
p_{24}^2 &= (t - (m_\rho - m_\pi)^2)(t - (m_\rho + m_\pi)^2)/4t \\
b(s) &= \{((s - s_-)(s - s_+) + sq^2m_\rho{}^2/m_\pi{}^2)^{1/2} + 2(s - q^2 - m_\pi{}^2)\} \\
&\quad \times (2m_\pi{}^2/(s - 4m_\pi{}^2)) + m_\pi{}^2.
\end{aligned} \tag{3.5}$$

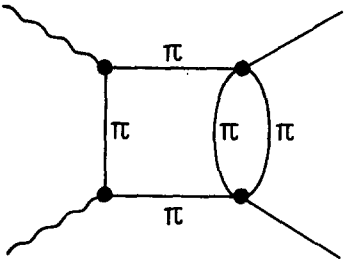

FIG. 2. Diagram which determines the boundary in the Khuri representation for ω exchange.

In the limit $q^2 \to 0$, $m_\rho^2 \to 0$ this reduces to the familiar form [8]

$$\xi(s) = \text{arc cosh}(1 + (s - 4m_\pi^2)(9s - 4m_\pi^2)/32sm_\pi^2).$$

With this form factor the partial wave projection of the ω exchange diagram is calculated numerically. The result will be called $t_{i\omega}^0(s)$, $i = 1, 2$, where

$$\begin{aligned} t_1^0 &= T_{11}^0 + T_{00}^0 \\ t_2^0 &= T_{11}^0 - T_{00}^0 . \end{aligned} \tag{3.6}$$

On the right-hand cut we assume unitarity with two-pion intermediate states, i.e.,

$$\text{Im } t_i^0(s) = e^{-i\delta_0(s)} \sin \delta_0(s)\, t_i^0(s) \tag{3.7}$$

where $\delta_0(s)$ is the $\pi\pi$ s-wave phase shift for $I = 0$. All other intermediate states are neglected. This should be a reasonable approximation at least up to around 1 GeV^2, in particular, since anomalous singularities will play a dominant role and higher intermediate states have less chance to aquire anomalous singularities compared to the two-pion intermediate state. The elastic $\pi\pi$ scattering amplitude $a_0(s)$ is written in the usual N/D form:

$$a_0(s) = (s/(s - 4m_\pi^2))^{1/2} e^{i\delta_0(s)} \sin \delta_0(s) = N(s)/D(s). \tag{3.8}$$

Under the condition that the left-hand cut L and the right-hand cut of $t_i^0(s)$ do not overlap we can fulfill the Eq. (3.7) by writing a dispersion relation for $t_i^0(s)\, D(s)$ over the left-hand cut:

$$t_i^0(s) = D^{-1}(s) \frac{1}{\pi} \int_L ds' \frac{D(s')\, \text{Im } t_i^0(s')}{s' - s} . \tag{3.9}$$

In (3.9) the amplitude $t_i^0(s)$ is expressed by $D(s)$ and the discontinuity of $t_i^0(s)$

over the left-hand cut L. As is well known, Eq. (3.9) can be transformed also into an integral over the right-hand cut: $4m_\pi^2 \leqslant s < \infty$. The result is:

$$t_i^0(s) - t_{iL}^0(s) = -D^{-1}(s)\frac{1}{\pi}\int_{4m_\pi^2}^{\infty} ds' \frac{\operatorname{Im} D(s')\, t_{iL}^0(s')}{s' - s} \tag{3.10}$$

where $t_{iL}^0(s)$ is given by (3.9) with $D = 1$. Of course (3.10) is the standard Omnes solution (9). The D-function can be calculated from the phase shift $\delta_0(s)$

$$D(s) = \exp\left\{-((s - s_0)/\pi)\int_{4m_\pi^2}^{\infty} ds' \,(\delta_0(s')/(s' - s_0)(s' - s))\right\} \tag{3.11}$$

where s_0 is arbitrary. We have $\operatorname{Im} D = -e^{i\delta_0}\sin\delta_0 D = -((s - 4m_\pi^2)/s)^{1/2} N$. Here we have left out the subtraction terms for ease of writing, and so we will do in the following. Including the subtraction terms (subtraction point s_0) Eqs. (3.9) and (3.10) would read

$$t_i^0(s) = \frac{s - s_0}{D(s)}\frac{1}{\pi}\int_L ds' \frac{D(s')\operatorname{Im} t_i^0(s')}{(s' - s)(s' - s_0)} + \frac{D(s_0)}{D(s)} t_{iL}^0(s_0) \tag{3.9a}$$

$$t_i^0(s) - t_{iL}^0(s) = -\frac{s - s_0}{D(s)}\frac{1}{\pi}\int_{4m_\pi^2}^{\infty} ds' \frac{t_{iL}^0(s')\operatorname{Im} D(s')}{(s' - s)(s' - s_0)}. \tag{3.10a}$$

Eq. (3.10) is valid if no anomalous thresholds are present. In the following part of this section we investigate how (3.9) or (3.10) are modified if anomalous thresholds occur in $t_i^0(s)$.

We start with the case, where the left-hand cut t_{iL}^0 is approximated by the one-pion exchange contribution $t_{i\pi}^0$.

First we study the analytic structure of $t_{i\pi}^0$. The partial waves for the one-pion exchange terms are calculated with the help of (3.2). The partial-wave projections of the invariant amplitudes (they are given in [7]) are obtained as

$$\begin{aligned} A_1{}^j &= -e g_{\rho\pi\pi} F_\pi(q^2)\, A^j \\ A_2{}^j &= 2e g_{\rho\pi\pi} F_\pi(q^2)\frac{1}{p_1{}^2 + q^2 - s} A^j \\ A_3{}^j &= A_4{}^j = A_5{}^j = 0 \end{aligned} \tag{3.12}$$

so that

$$\begin{aligned} A^j &= \frac{1}{2}\int_{-1}^{+1} d\cos\theta \left(\frac{1}{t - m_\pi^2} + \frac{1}{u - m_\pi^2}\right) P_j(\cos\theta) \\ &= -\frac{1}{2\,|\,\mathbf{p}_2\,|\,|\,\mathbf{q}\,|}\,(Q_j(z) + (-1)^j\, Q_j(-z)) \end{aligned} \tag{3.13}$$

with

$$z = \frac{s - p_1^2 - q^2}{4\,|\,\mathbf{p}_2\,|\,|\,\mathbf{q}\,|} = \frac{s^{1/2}(s - p_1^2 - q^2)}{(s - 4m_\pi^2)^{1/2}(s - s_+)^{1/2}(s - s_-)^{1/2}}\,.$$

Here s_+ is the threshold for the process $\gamma\rho^0 \to \pi^+\pi^-$ whereas in the reaction $\gamma \to \rho^0\pi^+\pi^-$ the variable s varies in the interval: $4m_\pi^2 \leqslant s \leqslant s_-$ with $s_\pm = ((q^2)^{1/2} \pm (p_1^2)^{1/2})^2$, $p_1^2 = m_\rho^2$. Except for the extra kinematic pole at $s = p_1^2 + q^2$ in A_2^j, which must cancel in the sum of all partial waves for pion exchange, the singularity structure of the partial waves is determined by the projections A^j in (3.13). For $s \geqslant s_+$ the partial-wave projection A^j is proportional to $Q_j(z)$ as given by (3.13), in particular for $j = 0$:

$$-A^0 = \frac{1}{|\,\mathbf{p}_2\,|\,|\,\mathbf{q}\,|}\,Q_0(z) = \frac{1}{2\,|\,\mathbf{p}_2\,|\,|\,\mathbf{q}\,|}\ln\frac{z+1}{z-1}\,. \tag{3.14}$$

For stable particles so that $0 \leqslant q^2 \leqslant 4m_\pi^2$ and $0 \leqslant m_\rho^2 \leqslant 4m_\pi^2$ and in absence of anomalous thresholds, i.e., for $q^2 + m_\rho^2 \leqslant 4m_\pi^2$ the expressions (3.13) or (3.14) can be continued to all complex s as usual. To reach the case $q^2 + m_\rho^2 > 4m_\pi^2$ which is the relevant case for $\gamma \to \rho\pi\pi$ where q^2 is above $(m_\rho + 2m_\pi)^2$ we start from (3.14) valid for $q^2 + m_\rho^2 \leqslant 4m_\pi^2$ and continue in m_ρ^2 and q^2. Problems of this sort have been solved before in connection with deuteron reactions where anomalous thresholds occur because of the small binding energy of the deuteron. Essentially we follow the methods developed for this case [10]. As a function of s the amplitude A^0 has branch point singularities at $s = 0$, $4m_\pi^2$ and $((q^2)^{1/2} \pm m_\rho)^2$, which come from the square roots in $|\,\mathbf{p}_2\,|$ and $|\,\mathbf{q}\,|$, and at points s for which

$$z = \pm 1 \tag{3.15}$$

To locate these latter singularities in the complex s plane we must solve (3.15). We shall do this and study the branch points as a function of m_ρ^2 and q^2. Let us start with the case of stable external particles, so that $0 \leqslant q^2 \leqslant 4m_\pi^2$ and $0 \leqslant m_\rho^2 \leqslant 4m_\pi^2$ with $q^2 + m_\rho^2 \leqslant 4m_\pi^2$ to avoid anomalous thresholds caused by bound states with small binding energies.

The roots of (3.15) are found from

$$as^2 + 2bs + c = 0 \tag{3.16}$$

where

$$\begin{aligned} a &= m_\pi^2 \\ 2b &= q^2 m_\rho^2 - 2m_\pi^2(q^2 + m_\rho^2) \\ c &= m_\pi^2(q^2 - m_\rho^2)^2. \end{aligned} \tag{3.17}$$

With $s = x + iy$ Eq. (3.16) is equivalent to

$$a(x^2 - y^2) + 2bx + c = 0 \tag{3.18}$$

$$y(ax + b) = 0. \tag{3.19}$$

So the singularities of (3.14) (and of the partial wave amplitudes) are given by the points of intersection of the hyperbolas (3.18) with the pair of straight lines $y = 0$ and $x = -b/a$. The hyperbola (Eq. 3.18)) intersects the straight line only if the discriminant $b^2 - ac \leqslant 0$. The discriminant is equal to

$$b^2 - ac = \tfrac{1}{4}q^2 m_\rho^2 (4m_\pi^2 - q^2)(4m_\pi^2 - m_\rho^2) \tag{3.20}$$

so that $b^2 - ac \geqslant 0$ for the case of stable external particles. Then the hyperbola intersects only the line $y = 0$ and we have two branch points lying on the real axis at points $s_{1,2}$ which are

$$as_{1,2} = -b \pm (b^2 - ac)^{1/2}. \tag{3.21}$$

These two points lie between s_- and $4m_\pi^2$. Equation (3.14) shows that A^0 is real in the intervals of the real axis: $x \in [0, s_-]$ and $x \in [4m_\pi^2, s_+]$ (see Fig. 3 for the transformation $s \to z(s)$), so that A^0 has cuts only for $-\infty \leqslant s \leqslant 0$ and $s_2 \leqslant s \leqslant s_1$. This cut structure is shown in Fig. 4. The corresponding representation, valid for stable external particles, therefore is

$$-\frac{1}{2}A^0 = \int_{-\infty}^{0} ds' \frac{1}{s' - s} \frac{(s')^{1/2}}{((s' - 4m_\pi^2)(s' - s_+)(s' - s_-))^{1/2}}$$

$$+ \int_{s_2}^{s_1} ds' \frac{1}{s' - s} \frac{(s')^{1/2}}{((s' - 4m_\pi^2)(s' - s_+)(s' - s_-))^{1/2}}. \tag{3.22}$$

Next we take a fixed value of $q^2 \leqslant 4m_\pi^2$ and $q^2 \leqslant m_\rho^2$, replace m_ρ^2 by $m_\rho^2 + i\epsilon$ (ϵ small and positive) in (3.21) and study the branch points as a function of m_ρ^2 with increasing m_ρ^2 starting from a value $m_\rho^2 \leqslant 4m_\pi^2$. For $m_\rho^2 \to m_\rho^2 + i\epsilon$ the branch points s_1 and s_2 lie above the real axis. If m_ρ^2 is increased s_1 and s_2 migrate parallel to the real axis towards $4m_\pi^2$ as is shown in Fig. 4. s_1 reaches $4m_\pi^2$ for $m_\rho^2 = 4m_\pi^2 - q^2$, and turns around $4m_\pi^2$, thereby crossing the right-hand cut and reaches the value $s = 4m_\pi^2 - q^2$ in the lower half plane if $m_\rho^2 = 4m_\pi^2$. s_2 then has the same value in the upper half plane, since the discriminant vanishes for $m_\rho^2 = 4m_\pi^2$ (see Eq. (3.20)). Increasing m_ρ^2 further the branch points s_1 and s_2 migrate into the complex plane ($s_1(s_2)$ in the lower (upper) half part), up to the points, where m_ρ^2 reaches its physical value, as shown in Fig. 4. Now we make q^2 complex by changing q^2 into $q^2 + i\eta$ ($\eta > 0$, η small) and increase q^2 from its

value below $4m_\pi^2$ up to $4m_\pi^2$. Then s_2 and s_1 approach the negative real axis from above and below, respectively. They meet at the point $s_1 = s_2 = 4m_\pi^2 - m_\rho^2$ (see Fig. 4). By increasing q^2 up to $q^2 = m_\rho^2$ the branch point s_1 migrates along the real axis to the left up to the point $s_1 = 4m_\rho^2 - m_\rho^4/m_\pi^2$ whereas s_2 recedes to the right up to $s_2 = 0$ (see Fig. 4, the endpoints of s_1, s_2, and s_- are shown as crosses). For $q^2 = m_\rho^2$ the branch cut between $s_2 = 0$ and s_1 disappears. s_2 is not a branch

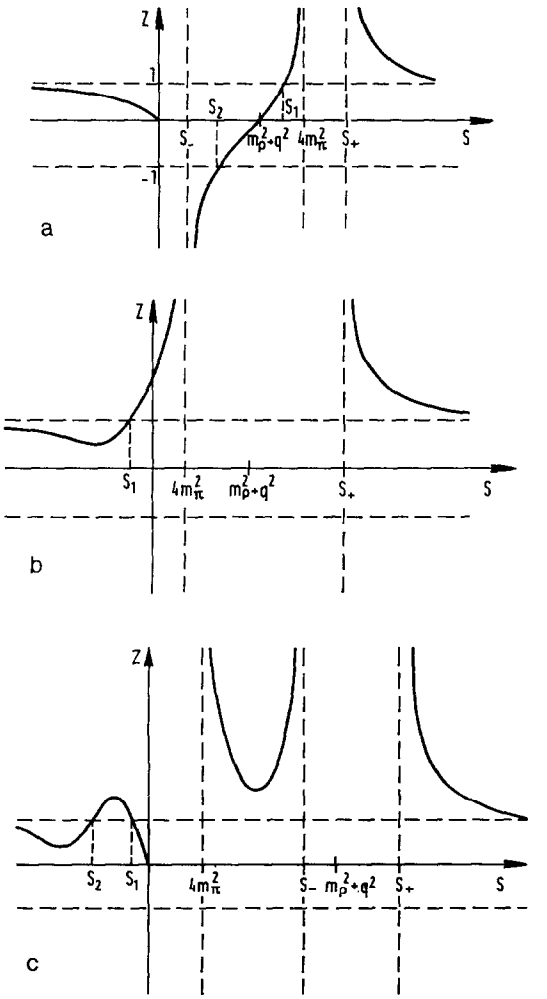

FIG. 3. Transformation $s \to z(s)$ for the three cases (a) $m_\rho^2 + q^2 \leqslant 4m_\pi^2$, (b) $m_\rho^2 = q^2 \geqslant 4m_\pi^2$, and (c) $q^2 > m_\rho^2$, $m_\rho^2 \geqslant 4m_\pi^2$, $q^2 \geqslant 4m_\pi^2$.

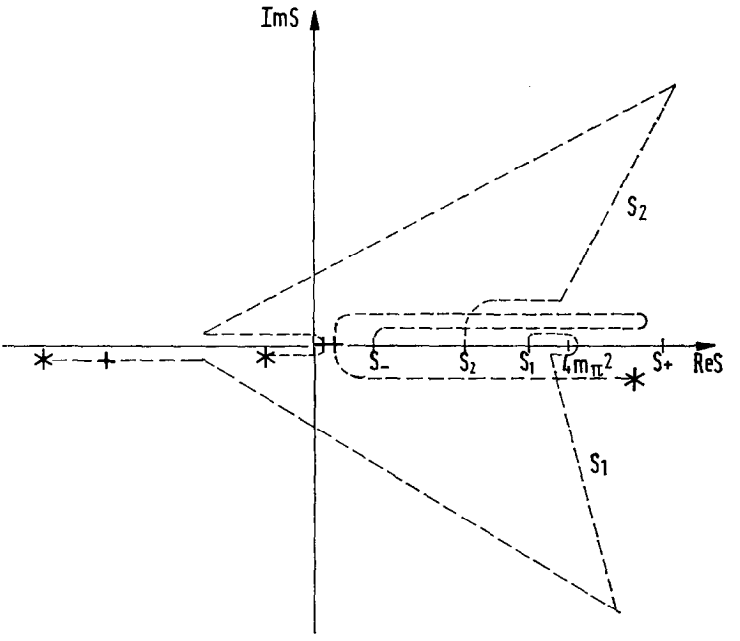

FIG. 4. Continuation of s_1, s_2, and s_- for increasing m_ρ^2 and q^2 up to values of physical interest for the π exchange diagram.

point anymore, as is seen in Fig. 3 where $z(s)$ is given as a function of s. Then A^0 has the following representation:

$$-\frac{1}{2}A^0 = \int_{-\infty}^{s_1} ds' \frac{1}{s'-s} \frac{1}{((s'-4m_\pi^2)(s'-4m_\rho^2))^{1/2}}$$
$$+ \int_{s_1}^{4m_\pi^2} ds' \frac{1}{s'-s} \frac{2}{((s'-4m_\pi^2)(s'-4m_\rho^2))^{1/2}}. \qquad (3.23)$$

The second integral on the right-hand side of (3.23) comes from the continuation in m_ρ^2 and q^2 and originates from the deformation of the integration path in connection with the endpoint s_1. The next step is to continue q^2 further up to values above the threshold for the production of $\rho\pi\pi$ final states, $q^2 \geqslant (m_\rho + 2m_\pi)^2$. Then s_2 turns around the point $s = 0$ and migrates to the left in the lower half plane whereas s_1 goes also to the left, the same distance parallel to the real axis. s_- crosses the positive real axis near the origin without crossing the path of s_2 and migrates to the right in the lower half plane (see Fig. 4, the endpoints of continuation are marked by a star). To write down the representation of A^0 in this case we must deform again the integration path connecting the branch point s_1.

Otherwise the location of the cuts is obtained from the transformation $s \to z(s)$ shown in Fig. 3. The representation for A^0 then is:

$$-\frac{1}{2}A^0 = \int_{-\infty}^{0} ds' \frac{1}{s'-s} \frac{(s')^{1/2}}{((s'-4m_\pi^2)(s'-s_+)(s'-s_-))^{1/2}}$$
$$-\int_{s_2}^{s_1} ds' \frac{1}{s'-s} \frac{(s')^{1/2}}{((s'-4m_\pi^2)(s'-s_+)(s'-s_-))^{1/2}}$$
$$-\int_{4m_\pi^2}^{s_-} ds' \frac{1}{s'-s} \frac{2(s')^{1/2}}{((s'-4m_\pi^2)(s'-s_-)(s'-s_+))^{1/2}}. \quad (3.24)$$

We see that for equal external masses $m_\rho^2 = q^2$ the representation (3.24) coincides with (3.23). A^0 now has an imaginary part in the physical region: $4m_\pi^2 \leqslant s \leqslant s_-$. It is clear that this term will dominate for $\gamma \to \rho\pi\pi$.

As the next step we incorporate the final state interaction in the s-channel. In the situation where $q^2 + m_\rho^2 \leqslant 4m_\pi^2$ and anomalous thresholds are absent the final state corrected solution for $-\frac{1}{2}A^0$ is given by (3.9). The discontinuity over the left-hand cut ($-\infty < s \leqslant 0$ and $s_2 \leqslant s \leqslant s_1$) can be read off from (3.22), so that the final result is

$$-\frac{1}{2}A^0 = \frac{1}{D(s)}\int_{-\infty}^{0} ds' \frac{1}{s'-s} \frac{(s')^{1/2}\,D(s')}{((s'-4m_\pi^2)(s'-s_+)(s'-s_-))^{1/2}}$$
$$+\frac{1}{D(s)}\int_{s_2}^{s_1} ds' \frac{1}{s'-s} \frac{(s')^{1/2}\,D(s')}{((s'-4m_\pi^2)(s'-s_+)(s'-s_-))^{1/2}}. \quad (3.25)$$

If m_ρ^2 and q^2 are increased we must continue (3.25) in the same way we did for A^0 without final state interaction. For example for $q^2 = m_\rho^2$ and $m_\rho^2 \geqslant 2m_\pi^2$ we obtain for A^0 the following representation instead of (3.23):

$$-\frac{1}{2}A^0 = \frac{1}{D(s)}\int_{-\infty}^{s_1} ds' \frac{1}{s'-s} \frac{D(s')}{((s'-4m_\pi^2)(s'-4m_\rho^2))^{1/2}}$$
$$+\frac{1}{D(s)}\int_{s_1}^{4m_\pi^2} ds' \frac{1}{s'-s} \frac{D(s')(1+e^{2i\delta_0(s')})}{((s'-4m_\pi^2)(s'-4m_\rho^2))^{1/2}}. \quad (3.26)$$

Similar to Eq. (3.9) we can transform (3.26) into integrals over the right-hand cut. The result is:

$$-\frac{1}{2}(A^0 - A_L^0) = -\frac{1}{D(s)}\frac{1}{\pi}\int_{4m_\pi^2}^{\infty} ds' \frac{(-(1/2)\,A_L^0(s'))\,\mathrm{Im}\,D(s')}{s'-s}$$
$$+\frac{1}{D(s)}\int_{s_1}^{4m_\pi^2} ds' \frac{1}{s'-s} \frac{2D(s')\sin\delta_0(s')\,e^{i\delta_0(s')}}{((s'-4m_\pi^2)(4m_\rho^2-s'))^{1/2}}. \quad (3.27)$$

In (3.27) the phase shift $\delta_0(s)$ must be contined below threshold. We have

$$D(s) \sin \delta_0(s)\, e^{i\delta_0(s)} = -\mathrm{Im}\, D(s) = ((s - 4m_\pi^2)/s)^{1/2}\, N(s). \tag{3.28}$$

Our Eq. (3.27) agrees with the result obtained by Mandelstam [10] and by Blankenbecler and Nambu [10] for the case of bound systems with small binding.

Similarly for $q^2 > (m_\rho + 2m_\pi)^2$ we include the final state interaction when the left-hand cut is given by (3.24). We obtain in this case:

$$\begin{aligned}
-\frac{1}{2}A^0 = {} & \frac{1}{D(s)}\int_{-\infty}^{0} ds' \frac{1}{s'-s} \frac{(s')^{1/2}\, D(s')}{((s'-4m_\pi^2)(s'-s_-)(s'-s_+))^{1/2}} \\
& - \frac{1}{D(s)}\int_{s_2}^{s_1} ds' \frac{1}{s'-s} \frac{(s')^{1/2}\, D(s')\, e^{2i\delta_0(s')}}{((s'-4m_\pi^2)(s'-s_-)(s'-s_+))^{1/2}} \\
& - \frac{1}{D(s)}\int_{4m_\pi^2}^{s_-} ds' \frac{1}{s'-s} \frac{(s')^{1/2}\, D(s')(1 + e^{2i\delta_0(s')})}{((s'-4m_\pi^2)(s'-s_-)(s'-s_+))^{1/2}} \\
& + \frac{1}{D(s)}\int_{s_2}^{0} ds' \frac{1}{s'-s} \frac{(s')^{1/2}\, D(s')(1 - e^{2i\delta_0(s')})}{((s'-4m_\pi^2)(s'-s_-)(s'-s_+))^{1/2}} \\
& - \frac{1}{D(s)}\int_{0}^{4m_\pi^2} ds' \frac{1}{s'-s} \frac{(s')^{1/2}\, D(s')(1 - e^{2i\delta_0(s')})}{((s'-4m_\pi^2)(s'-s_-)(s'-s_+))^{1/2}}\,.
\end{aligned} \tag{3.29}$$

It is clear that (3.29) reduces to (3.24) if the $\pi\pi$ interaction vanishes ($D = 1$, $\delta_0 = 0$). If we transform (3.29) into integrals over the right-hand cut we have

$$\begin{aligned}
-\frac{1}{2}(A^0 - A_L^0) = {} & -\frac{1}{D(s)}\frac{1}{\pi}\int_{4m_\pi^2}^{\infty} ds' \frac{(-(1/2)\, A_L^0(s'))\, \mathrm{Im}\, D(s')}{s'-s} \\
& - \frac{1}{D(s)}\int_{4m_\pi^2}^{s_-} ds' \frac{1}{s'-s} \frac{2(s')^{1/2}\, i \sin\delta_0(s')\, e^{i\delta_0(s')} D(s)}{((s'-4m_\pi^2)(s'-s_-)(s'-s_+))^{1/2}} \\
& - \frac{1}{D(s)}\int_{s_2}^{s_1} ds' \frac{1}{s'-s} \frac{2(s)^{1/2}\, i \sin\delta_0(s')\, e^{i\delta_0(s')} D(s')}{((s'-4m_\pi^2)(s'-s_-)(s'-s_+))^{1/2}} \\
& - \frac{1}{D(s)}\int_{s_2}^{0} ds' \frac{1}{s'-s} \frac{2(s')^{1/2}\, i \sin\delta_0(s')\, e^{i\delta_0(s')} D(s')}{((s'-4m_\pi^2)(s'-s_-)(s'-s_+))^{1/2}} \\
& - \frac{1}{D(s)}\int_{0}^{4m_\pi^2} ds' \frac{1}{s'-s} \frac{2(s')^{1/2}\, i \sin\delta_0(s')\, e^{i\delta_0(s')} D(s')}{((s'-4m_\pi^2)(s'-s_-)(s'-s_+))^{1/2}}\,.
\end{aligned} \tag{3.30}$$

Since we have no information about the continuation of the phase shift below the $\pi\pi$ threshold we shall neglect the last three terms in (3.30). The inclusion of subtraction terms is straightforward.

Concerning anomalous threshold terms, the pion exchange is the most important one. For all other states in the t and u channel with larger masses, as for example the ω, which make the ρ stable, the situation is simpler as for the pion intermediate state as we shall see.

In the following we shall now consider the ω exchange, especially the continuation of the partial wave amplitudes as a function of q^2. Here the partial wave projections of the invariant amplitudes are [7]

$$\begin{aligned}
A_1{}^j &= -\frac{1}{8} g_{\rho\omega\pi} g_{\gamma\omega\pi}(q^2) \frac{1}{2}\int_{-1}^{1} d\cos\theta \\
&\quad \times \left(\frac{4t + 4m_\pi{}^2 - s - p_1{}^2 - q^2}{t - m_\omega{}^2} + \frac{4u + 4m_\pi{}^2 - s - p_1{}^2 - q^2}{u - m_\omega{}^2}\right) P_j(\cos\theta) \\
A_2{}^j &= A_5{}^j = \frac{1}{4} g_{\rho\omega\pi} g_{\gamma\omega\pi}(q^2) \frac{1}{2}\int_{-1}^{1} d\cos\theta \left(\frac{1}{t - m_\omega{}^2} + \frac{1}{u - m_\omega{}^2}\right) P_j(\cos\theta) \\
A_3{}^j &= A_4{}^j = -\frac{1}{4} g_{\rho\omega\pi} g_{\gamma\omega\pi}(q^2) \frac{1}{2}\int_{-1}^{1} d\cos\theta \left(\frac{1}{t - m_\omega{}^2} - \frac{1}{u - m_\omega{}^2}\right) P_j(\cos\theta).
\end{aligned} \tag{3.31}$$

Let us depict one of the partial wave amplitudes free of kinematical singularities, e.g., A^0. A^0 now is given instead of (3.13) by:

$$A^0 = \frac{1}{2}\int_{-1}^{1} d\cos\theta \left(\frac{1}{t - m_\omega{}^2} + \frac{1}{u - m_\omega{}^2}\right) = -\frac{1}{|\mathbf{p}_2||\mathbf{q}|} Q_0(z) \tag{3.32}$$

with

$$z = (s - p_1{}^2 - q^2 + 2(m_\omega{}^2 - m_\pi{}^2))/4\,|\mathbf{p}_2||\mathbf{q}| \tag{3.33}$$

The singularities in s, which correspond to $z = \pm 1$, are found from (3.16), where a, b and c are now given by:

$$\begin{aligned}
a &= m_\omega{}^2 \\
2b &= m_\omega{}^4 - m_\omega{}^2(2m_\pi{}^2 + q^2 + m_\rho{}^2) + (m_\pi{}^2 - q^2)(m_\pi{}^2 - m_\rho{}^2) \\
c &= m_\pi{}^2(q^2 - m_\rho{}^2)^2
\end{aligned} \tag{3.34}$$

The discriminant $b^2 - ac$ is for this case equal to

$$\begin{aligned}
b^2 - ac &= \tfrac{1}{4}((m_\omega + m_\pi)^2 - q^2)(q^2 - (m_\omega - m_\pi)^2) \\
&\quad \times ((m_\omega + m_\pi)^2 - m_\rho{}^2)(m_\rho{}^2 - (m_\omega - m_\pi)^2)
\end{aligned} \tag{3.35}$$

so that $b^2 - ac \geqslant 0$ for the case of stable particles, i.e., $(m_\omega - m_\pi)^2 < m_\rho{}^2 < (m_\omega + m_\pi)^2$ and $(m_\omega - m_\pi)^2 \leqslant q^2 \leqslant (m_\omega + m_\pi)^2$. The physical ρ mass is such that

this constraint for m_ρ^2 is satisfied so that only q^2 must be continued up to the range of physical interest. For the constraint on q^2 above we have two branch points $s_{1,2}$ on the real axis given by

$$as_{1,2} = -b \pm (b^2 - ac)^{1/2}. \tag{3.36}$$

For $q^2 = (m_\omega - m_\pi)^2$ the two branch points coincide and lie below $2m_\pi^2$ on the real axis. As before we give q^2 a small imaginary part and study the branch points as a function of q^2. The migration of s_1, s_2, and s_- as a function of q^2 is shown in Fig. 5. For $q^2 = 2(m_\omega^2 + m_\pi^2) - m_\rho^2$ the branch point crosses the physical cut $s \geqslant 4m_\pi^2$ and migrates into the lower half plane to the left up to the point $s = s_0$ where s_1 and s_2 start to migrate into the complex plane, when $q^2 = (m_\omega + m_\pi)^2$. Below the critical point $q^2 + m_\rho^2 = 2(m_\omega^2 + m_\pi^2)$ the s-wave amplitude A^0 has the same representation as for pion exchange as given by (3.22). The corresponding final state corrected amplitude is then equal to (3.25), of course with the integration limits s_1 and s_2 as obtained for ω exchange. If q^2 is increased up to the value of interest we have to correct for the fact of s_1 and s_2 migrate into the complex plane. The result is:

$$\begin{aligned}
-\frac{1}{2}A^0 = &\int_{-\infty}^{0} ds' \frac{1}{s'-s} \frac{(s')^{1/2}}{((s'-4m_\pi^2)(s'-s_-)(s'-s_+))^{1/2}} \\
&+ \int_{s_2}^{s_0} ds' \frac{1}{s'-s} \frac{(s')^{1/2}}{((s'-4m_\pi^2)(s'-s_-)(s'-s_+))^{1/2}} \\
&+ \int_{s_0}^{s_1} ds' \frac{1}{s'-s} \frac{(s')^{1/2}}{((s'-4m_\pi^2)(s'-s_-)(s'-s_+))^{1/2}} \\
&- \int_{4m_\pi^2}^{s_-} ds' \frac{1}{s'-s} \frac{2(s')^{1/2}}{((s'-4m_\pi^2)(s'-s_-)(s'-s_+))^{1/2}}.
\end{aligned} \tag{3.37}$$

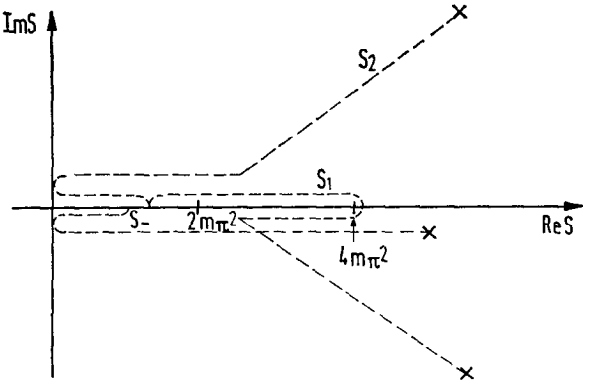

FIG. 5. Continuation of s_1, s_2, and s_- for the ω exchange diagram.

Based on (3.37) the final-state corrected amplitude is:

$$
\begin{aligned}
-\frac{1}{2}A^0 = {} & \frac{1}{D(s)}\int_{-\infty}^{0} ds' \frac{1}{s'-s} \frac{(s')^{1/2}\,D(s')}{((s'-4m_\pi^2)(s'-s_-)(s'-s_+))^{1/2}} \\
& + \frac{1}{D(s)}\int_{s_2}^{s_0} ds' \frac{1}{s'-s} \frac{(s')^{1/2}\,D(s')}{((s'-4m_\pi^2)(s'-s_-)(s'-s_+))^{1/2}} \\
& + \frac{1}{D(s)}\int_{s_0}^{s_1} ds' \frac{1}{s'-s} \frac{(s')^{1/2}\,D(s')\,e^{2i\delta_0(s')}}{((s'-4m_\pi^2)(s-s_-)(s-s_+))^{1/2}} \\
& - \frac{1}{D(s)}\int_{4m_\pi^2}^{s_-} ds' \frac{1}{s'-s} \frac{(s')^{1/2}\,D(s')(1+e^{2i\delta_0(s')})}{((s'-4m_\pi^2)(s'-s_-)(s'-s_+))^{1/2}} \\
& + \frac{1}{D(s)}\int_{s_0}^{4m_\pi^2} ds' \frac{1}{s'-s} \frac{(s')^{1/2}\,D(s')(1-e^{2i\delta_0(s')})}{((s'-4m_\pi^2)(s'-s_-)(s'-s_+))^{1/2}}\,.
\end{aligned}
\tag{3.38}
$$

Of course (3.38) agrees with (3.37) for vanishing final state interaction. It is convenient to transform the result (3.38) in such a way that mostly integrals over the right-hand cut appear. We denote the uncorrected amplitude (3.37) by A_L^0 and obtain:

$$
\begin{aligned}
-\frac{1}{2}(A^0 - A_L^0) = {} & -\frac{1}{D(s)}\frac{1}{\pi}\int_{4m_\pi^2}^{\infty} ds' \frac{(-(1/2)\,A_L^0(s'))\,\mathrm{Im}\,D(s')}{s'-s} \\
& - \frac{1}{D(s)}\int_{4m_\pi^2}^{s_-} ds' \frac{1}{s'-s} \frac{2(s')^{1/2}\,D(s')\,i\sin\delta_0(s')\,e^{i\delta_0(s')}}{((s'-4m_\pi^2)(s'-s_-)(s'-s_+))^{1/2}} \\
& + \frac{1}{D(s)}\int_{s_0}^{s_1} ds' \frac{1}{s'-s} \frac{2(s')^{1/2}\,D(s')\,i\sin\delta_0(s')\,e^{i\delta_0(s')}}{((s'-4m_\pi^2)(s'-s_-)(s'-s_+))^{1/2}} \\
& - \frac{1}{D(s)}\int_{0}^{4m_\pi^2} ds' \frac{1}{s'-s} \frac{2(s')^{1/2}\,D(s')\,i\sin\delta_0(s')\,e^{i\delta_0(s')}}{((s'-4m_\pi^2)(s'-s_-)(s'-s_+))^{1/2}}\,.
\end{aligned}
\tag{3.39}
$$

The last two integrals will be neglected since we have no information about the phase shift $\delta_0(s)$ outside the physical region. One should mention that the integrals in Eqs. (3.30) and (3.39) are finite at $s = s_-$ and $s = 4m_\pi^2$ even though it seems they are not. For this we remember that the last three integrals in Eqs. (3.30) and (3.39) proceed along the lower rim of the cut.

4. Results

Before presenting the results for the $\rho^0\epsilon$ transition form factors G_1 and G_2 we shall put together the input parameters. We need values for $g_{\rho\pi\pi}$, $g_{\rho\omega\pi}$, the form factors $F_\pi(q^2)$ and $g_{\gamma\omega\pi}(q^2)$ and the Regge trajectory α_ω. The coupling constants are chosen as follows $g_{\rho\pi\pi} = 5.97$, $g_{\rho\omega\pi} = 2.1 m_\pi^{-1}$, $g_{\gamma\omega\pi}(0) = 0.112 m_\pi^{-1}$ with $m_\rho = 0.77$ GeV. The form factor of the pion is approximated by the ρ dominance form

$$F_\pi(q^2) = m_\rho^2/(m_\rho^2 - q^2) \tag{4.1}$$

which gives a fairly good representation of the pion form factor in the space and timelike region [11]. The $\omega\pi$ transition form factor is also assumed to be given by the ρ dominance form

$$g_{\gamma\omega\pi}(q^2) = g_{\gamma\omega\pi}(0)(m_\rho^2/(m_\rho^2 - q^2)) \tag{4.2}$$

with $g_{\gamma\omega\pi}(0)$ fitted to the partial decay width $\Gamma(\omega \to \pi\gamma) = 0.9$ MeV. $g_{\rho\omega\pi}$ is obtained from $g_{\gamma\omega\pi}(0)$ through the usual ρ dominance extrapolation. This is a reasonable assumption here since anomalous singularities are not to be expected in this case.

The ω Regge trajectory is chosen to be $\alpha_\omega(t) = 0.5 + t$. These definitions completely specify our left-hand cut parametrization. For the right-hand cut we need the $\pi\pi$ s-wave shift. There exist many phase shift analysis for the $\pi\pi$ s-wave, which, unfortunately, are not unambiguous. On the other hand it seems to be established now that the s-wave phase shift goes through 90° under the ρ and the f mesons (12). The change of phase is rather slow and inelastic effects near the KK threshold are certainly present. Therefore one is reluctant to describe the behavior of the s-wave phase shift by T-matrix poles. To obtain a realistic description of the $\pi\pi$ s-wave, a many channel representations should be used. Then besides the process $\gamma \to \rho\pi\pi$ we had to consider also other processes as for example $\gamma \to \rho K\bar{K}$ which are coupled to $\rho\pi\pi$ via K^* exchange. Such many channel calculations would be beyond the scope of this paper [13]. Here we take for the $I = 0$ s-wave shift a simple Breit–Wigner ansatz

$$\delta_0(s) = \operatorname{arc\,cot}((m_\epsilon^2 - s)/\rho(s)\, Q_\epsilon) \tag{4.3}$$

where

$$\begin{aligned} \rho(s) &= (s - 4m_\pi^2)/s)^{1/2} \\ Q_\epsilon &= \Gamma_\epsilon m_\epsilon/\rho(m_\epsilon^2). \end{aligned} \tag{4.4}$$

The parameters m_ϵ and Γ_ϵ are $m_\epsilon = 0.7$ GeV and $\Gamma_\epsilon = 3m_\pi$.

With the parametrization described above we calculated the $\rho^0\epsilon$ transition form factor G_1 and G_2 with the help of Eq. (2.11). We considered three cases: (a) π and

ω exchange is assumed and the contributions of the anomalous singularities are fully taken into account, (b) only the π exchange contribution is taken into account instead of $\pi + \omega$ in (a), (c) the contributions coming from anomalous threshold singularities are neglected, but both exchanges π and ω are considered. The results are shown in Table I. Instead of G_2 we give the results for

$$\tilde{G}_2 = ((p_1q)^2 - p^2q^2)\, G_2/p_1q \tag{4.5}$$

so that $\tilde{G}_2$ has the same dimension as G_1. Both are given in units of m_π^{-1}. The numbers of G_1 and $\tilde{G}_2$ are such that $F_\pi(q^2)$ as given by Eq. (4.1) has been factored out. Therefore to obtain the actual form factors, G_1 and $\tilde{G}_2$ in Table 1 must be multiplied by $F_\pi(q^2)$. From Eq. (2.7) we see that the longitudinal cross section $\sigma_L \sim |\Gamma^0|^2$ is proportional to G_1^2, whereas the unpolarized transverse cross section $\sigma_U \sim |\Gamma^1|^2$ is proportional to $(G_1 + \tilde{G}_2)^2$. Without anomalous threshold contributions the form factors G_1 and $G_1 + \tilde{G}_2$, which determine the independent cross sections σ_L and σ_U are rather small. These cross sections are exhibited in Fig. 6c. Near threshold they are of the order of 0.1 nb, which is much to small compared to the measured cross section for $\sigma(e^+e^- \to 2\pi^+2\pi^-)$. Including anomalous thresholds the form factors G_1 and $\tilde{G}_2$ are much larger, in particular G_1 which contributes to both cross sections σ_U and σ_L, whereas $\tilde{G}_2$ seems to be less dependent on the inclusion of anomalous threshold terms. The comparison of the column (a) and (b) of Table I shows the influence of the ω exchange. It reduces $\tilde{G}_2$ for larger q^2 which has the effect that the cross section σ_U with π and ω exchange is larger for

TABLE I

Transition Form Factors G_1 and $\tilde{G}_2$ divided by F_π as a Function of q^2 for Three Cases

		1[a]		2[b]		3[c]	
q^2 $[m_\pi^2]$	q^2 [GeV^2]	G_1	$\tilde{G}_2$	G_1	$\tilde{G}_2$	G_1	$\tilde{G}_2$
100	1.96	0.222	−0.0832	0.198	−0.0388	0.0309	−0.0604
150	2.94	0.282	−0.0849	0.256	−0.0620	0.0329	−0.0568
175	3.43	0.308	−0.0893	0.283	−0.0786	0.0431	−0.0561
200	3.92	0.353	−0.0911	0.306	−0.0932	0.0545	−0.0565
300	5.88	0.475	−0.159	0.387	−0.157	0.100	−0.111
500	9.80	0.554	−0.113	0.505	−0.264	0.115	−0.0808
800	15.7	0.631	−0.0839	0.630	−0.390	0.124	−0.0546

[a] $\pi + \omega$ exchange with anomalous threshold contributions (atc). G_1 and $\tilde{G}_2$ are given in m_π^{-1}.

[b] π exchange with atc.

[c] $\pi + \omega$ exchange with atc neglected.

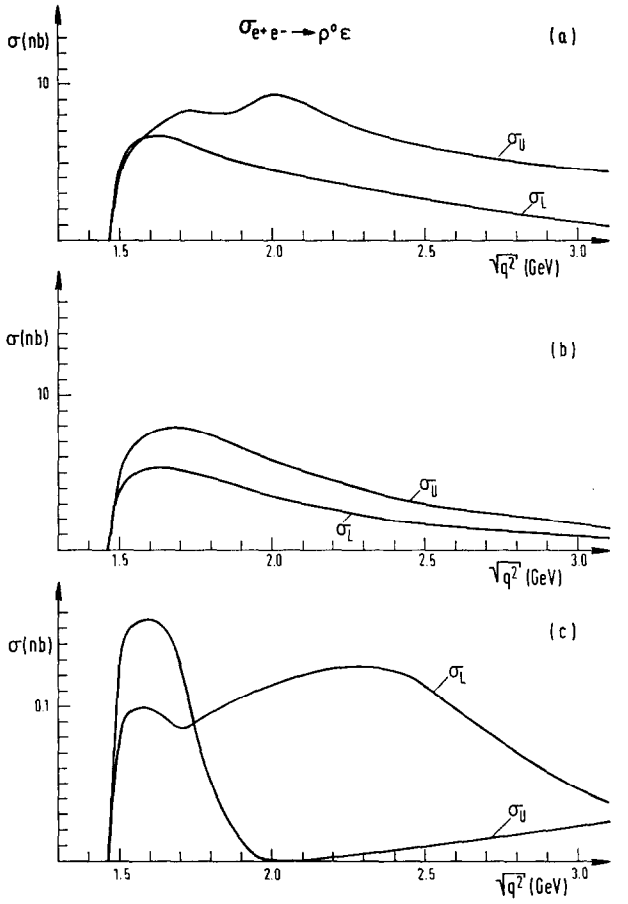

FIG. 6. Cross sections σ_U and σ_L for $e^+e^- \to \rho^0\epsilon$ as a function of the total cm energy $(q^2)^{1/2}$ for the three cases (a) π and ω exchange, (b) π exchange, and (c) π and ω exchange without contribution from anomalous thresholds.

higher q^2 than the cross section σ_U with π exchange only. Furthermore the inclusion of the ω causes a second maximum in σ_U near $(q^2)^{1/2} = 2$ GeV. σ_L is much less influenced by the ω exchange (see Fig. 6a and b).

In Fig. 7 we compared the calculated cross sections for the two cases (a) and (b) with the recent data of Bernadini *et al.* [14] and Mehrgardt *et al.* [15]. These data are for $e^+e^- \to \pi^+\pi^-\pi^+\pi^-$. The analysis shows that the dominant part are $\rho^0\pi^+\pi^-$ states. We assume that $\rho^0\pi^+\pi^-$ is dominantly $\rho^0\epsilon$. To account for the decay $\epsilon \to 2\pi^0$ the cross sections $\sigma = \sigma_U + \sigma_L$ in Fig. 6a and Fig. 6b must be multiplied by $\frac{2}{3}$ to obtain the $\rho^0\pi^+\pi^-$ channel. The agreement with the experimental data is

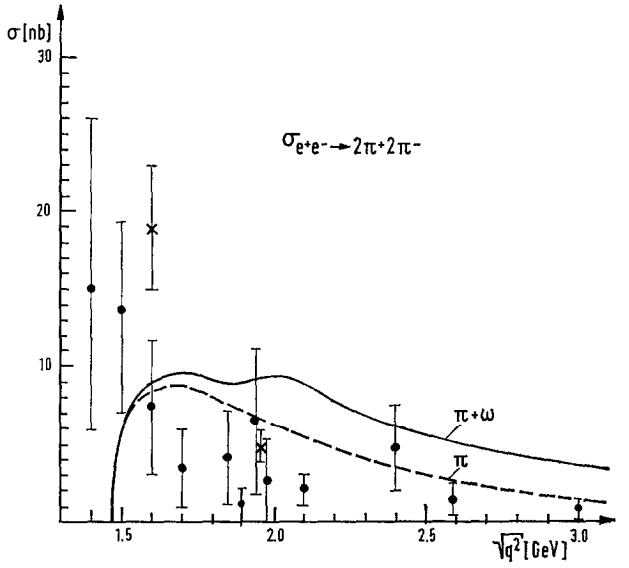

FIG. 7. Comparison of the theoretical prediction with the data of [14, 15] as a function of the total cm energy q^2. The curves show $\frac{2}{3}\sigma(e^+e^- \to \rho^0\epsilon)$.The dashed curve if for the π exchange model, the full curve is for the $\pi + \omega$ exchange model. The full points are the data of Bernadini *et al.* [14], the two cross points come from Mehrgardt *et al.* [15].

reasonable. The model with only π exchange agrees even better (version (b)) than the $\pi + \omega$ exchange model. In both models the fall-off of the form factors with increasing q^2 is not strong enough. Furthermore the threshold region is not well accounted for. This may be caused by the quasi-two-body approximation of the $\rho^0\pi^+\pi^-$ state. If the final state is treated as a genuine three-body state the cross section near threshold increases and the threshold is shifted to lower energies [7]. It may be that this effect is not sufficient to bring the theory into agreement with the data. In the moment we cannot exclude the possibility that a ρ' (1.6) is needed to explain the large cross section near threshold. Nevertheless we see that a reasonable interpretation of the Frascati data for $e^+e^- \to 2\pi^+\pi^-$ can be achieved by assuming the dominance of the $\rho^0\epsilon$ quasi-two-body final state and with our dispersion theoretic model of $\rho^0\epsilon$ transition form factor. Of course we can give a similar interpretation to the four-pion enhancement in the photoproduction process $\gamma p \to 2\pi^+2\pi^-p$ observed at SLAC [2]. It was essential to include the anomalous threshold contributions into the left-hand cut to obtain the right order of magnitude for the form factors G_1 and G_2 to fit the $e^+e^- \to 2\pi^+2\pi^-$ data. On the other hand the agreement with these data is not perfect (see Fig. 7). In particular the ω exchange contribution needs further study. Second the inclusion of other

exchanges, like for example A_1-exchange, might improve the large q^2 behavior of the form factors. Another problem is the inelasticity of the $\pi\pi$ s-wave, already mentioned, which might also modify our result. The study of all these effects is left for the future now where the basic mechanism has been established.

5. Conclusions

We conclude that anomalous thresholds play a dominant role in timelike q^2-leptoproduction of hadrons which makes any vector-dominance extrapolation into this regime rather doubtful. In the particular channel under consideration the effect is most significant at medium q^2 where the anomalous singularity contributions account for 98 % of the cross section. At higher q^2 this fraction reduces somewhat but the anomalous singularity contributions still stay dominant. One wonders why the naive vector dominance extrapolation of the $\epsilon\gamma\gamma$ coupling constant in [7] gave the correct order of magnitude for the $e^+e^- \to \rho^0\epsilon$ cross section. The reason is, that the actual $\epsilon\gamma\gamma$ coupling constant neglecting anomalous singularities would decrease as $q^2 = p_1^2 \to m_\rho^2$ in addition to the vector dominance corrections due to the fact that the left hand cut integral (Eq. (3.22)) starts at $s_1 = (-m_\rho^4 + 4m_\pi^2 m_\rho^2)/m_\pi^2$ instead of $s_1 = 0$ which has not been taken into account in [7]. It is the contribution from the anomalous thresholds which compensates this decrease so that the naive vector dominance extrapolation looks correct. If (say) q^2 is increased further (but $p_1 = m_\rho^2$ fixed) then the coupling constants (see Table I) start to increase again since in this regime kinematic factors (involving q^2) become important.

The dominance of anomalous singularities makes the dispersion relation approach a rather clean model for describing exclusive channels in electron–positron annihilation into hadrons. First of all the left-hand cut is well saturated by the exchange of a few light particles giving rise to anomalous thresholds. Secondly, intermediate states higher than two pions are unlikely to acquire anomalous singularities so that they can be ignored. This makes electron-positron annihilation into hadrons also extremely suitable for studying $\pi\pi$ scattering. Finally, we have achieved a fairly good description of the $e^+e^- \to \rho\pi\pi$ cross section.

We should mention that similar anomalous threshold effects are to be expected in form factors of other unstable particles, like for instance $\rho^+\rho^-$ (π exchange), $\Delta\bar{\Delta}$ (N— exchange) and many others. After completion of this work we learned that a calculation of the $\rho^0\epsilon$ electromagnetic form factor was done by Gutbrod and Weiss [15] based on a more field-theoretic model. The assumptions and the methods used in this calculation are completely different, although the final results agree qualitively with ours.

APPENDIX A

Here we list the transformation coefficients $g^i_{\lambda_1\kappa}$ defined in (2.4), which relate the s-channel helicity matrix elements to the invariant amplitudes $A_i(s, t)$ (see (2.3)):

$$g^1_{11} = -qp_1$$

$$g^2_{11} = 2qp_1\mathbf{p}_2^2 \sin^2\theta - Qq\,Qp_1$$

$$g^3_{11} = -q^2p_1Q$$

$$g^4_{11} = -p_1^2qQ$$

$$g^5_{11} = -p_1^2q^2$$

$$g^1_{1-1} = g^3_{1-1} = g^4_{1-1} = g^5_{1-1} = 0$$

$$g^2_{1-1} = -2qp_1\mathbf{p}_2^2 \sin^2\theta$$

$$g^1_{10} = g^4_{10} = g^5_{10} = 0$$

$$g^2_{10} = -2(2)^{1/2}(q^2)^{1/2}\,\mathbf{p}_2^2 \sin\theta\cos\theta$$

$$g^3_{10} = -2^{1/2}(q^2)^{1/2} \mid \mathbf{p}_2 \mid \mid \mathbf{q} \mid (p_{10} - q_0)\sin\theta$$

$$g^1_{01} = g^3_{01} = g^5_{01} = 0$$

$$g^2_{01} = -2(2)^{1/2}(p_1^2)^{1/2}\,\mathbf{p}_2^2 \sin\theta\cos\theta$$

$$g^4_{01} = -2^{1/2}(p_1^2)^{1/2} \mid \mathbf{p}_2 \mid \mid \mathbf{q} \mid (q_0 - p_{10})\sin\theta$$

$$g^1_{00} = -(q^2p_1^2)^{1/2}$$

$$g^2_{00} = 4(q^2p_1^2)^{1/2}\,\mathbf{p}_2^2 \cos^2\theta$$

$$g^3_{00} = 2(q^2p_1^2)^{1/2} \mid \mathbf{p}_2 \mid \mid \mathbf{q} \mid \cos\theta$$

$$g^4_{00} = 2(q^2p_1^2)^{1/2} \mid \mathbf{p}_2 \mid \mid \mathbf{q} \mid \cos\theta$$

$$g^5_{00} = -(q^2p_1^2)^{1/2}\,qp_1\,.$$

θ is the angle between $\mathbf{q}$ and $\mathbf{p}_2$ in the two-pion center-of-mass system. The variables $\mid \mathbf{q} \mid = \mid \mathbf{q}_1 \mid$, $\mid \mathbf{p}_2 \mid$, p_{10} and q_0 can all be expressed by $s = (q - p_1)^2$. The other Mandelstam invariants are $t = (q - p_2)^2 = m_\pi^2 + q^2 - 2q_0p_{20} + 2 \mid \mathbf{q} \mid \mid p_2 \mid \cos\theta$ and $u = (q - p_3)^2 = -s - t + q^2 + m_\rho^2 + 2m_\pi^2$. Furthermore $Q = p_2 - p_3$.

ACKNOWLEGMENT

We thank F. Gutbrod for discussion on his work.

REFERENCES

1. B. BARTOLI *et al.*, *Nuovo Cimento* **70** (1970), 615; *Phys. Rev.* **D6** (1972), 2374; G. BARBARINO *et al.*, *Nuovo Cimento Lett.* **3** (1972), 689; B. BORGIA *et al.*, *Nuovo Cimento* **13A** (1973), 593; F. CERADINI *et al.*, *Phys. Lett.* **43B** (1973), 341; B. RICHTER, Report at the Conf. on Lepton-Induced Reactions, Irvine, December 1973; W. CHINOWSKY, Lecture at the 4th International Conference on Experimental Meson Spectroscopy, Boston Mass., April 26–27, 1974.
2. P. SCHACHT *et al.*, preprint, Max-Planck Institut für Physik und Astrophysik, München; H. H. BINGHAM *et al. Phys. Lett.* **41B** (1972), 635; For a recent review see K. C. MOFFEIT, Proceedings of the 6th International Symposium on Electron and Photon Interaction at High Energies, Bonn, August 27–31, 1973.
3. A. BRAMON AND M. GRECO, *Nuovo Cimento Lett.* **3** (1972), 693; and the papers in [1, 2].
4. D. MORTARA, preprint, University of Illinois, october 1972; T. FERBEL AND P. SLATTERY, preprint, University of Rochester, COO-3065-40, 1973.
5. G. KRAMER, J. L. URETSKY, AND T. F. WALSH, *Phys. Rev.* **D3** (1971), 719; J. LAYSSAC AND F. M. RENARD, *Nuovo Cimento Lett.* **1** (1971), 197; *Nuovo Cimento* **6** (1971), 134; **10** (1972), 407; A. M. ALTOKHOV AND I. B. KHRIPLOVICH, *Sov. J. Nucl. Phys.* **13** (1971), 351; G. KRAMER, 1972 Cern School Lectures, Grado, May, 1972.
6. G. KRAMER AND T. F. WALSH, *Z. Phys.* **263** (1973), 361.
7. A. C. HIRSCHFELD AND G. KRAMER, *Nucl. Phys.* **B74** (1974), 211.
8. G. SCHIERHOLZ AND K. SUNDERMEYER, *Nucl. Phys.* **B40** (1972), 125, see also B. SCHREMPP-OTTO, F. SCHREMPP, AND T. F. WALSH, *Phys. Lett.* **36B** (1971), 463.
9. R. OMNES, *Nuovo Cimento* **8** (1958), 316.
10. R. OEHME, *Nuovo Cimento* **13** (1959), 778; *Phys. Rev.* **121** (1961), 1840; S. MANDELSTAM, *Phys. Rev. Lett.* **4** (1960), 84; R. BLANKENBECLER AND Y. NAMBU, *Nuovo Cimento* **18** (1960), 595; I. T. DRUMMOND, *Phys. Rev.* **140** (1965), 482.
11. M. BERNARDINI *et al.*, *Phys. Lett.* **46B** (1973), 261.
12. G. GRAYER *et al.*, Proceedings Third International Conference on Experimental Meson Spectroscopy, Philadelphia, 1972 (AIP Conf. Proc. No. 8, Particles and Fields Subseries No. 3, p. 5; J. T. CARROLL *et al.*, *Phys. Rev. Lett.* **28** (1972), 318.
13. See K. SUNDERMEYER, Desy report (Desy 74/17) for such a coupled channel analysis of $\gamma\gamma \to \pi\pi$ and $\gamma\gamma \to K\bar{K}$ for real photons.
14. M. BERNARDINI *et al.*, *Phys. Lett.* **53B** (1974), 384.
15. H. MEHRGARDT, P. WALOSCHEK, H. J. WILLUTZKI, G. WINTER, AND E. IAROCCI, preprint, unpublished; see also F. FELICETTI, Proceedings of the XVIIth International Conference on High Energy Physics, p. IV 10. London, 1974.
16. F. GUTBROD AND U. WEISS, A Model for the Process $e^+e^- \to \rho^0\epsilon$. Contribution to the Stanford Conference, August 1975; DESY report DESY 75/43.